

PDF hosted at the Radboud Repository of the Radboud University Nijmegen

The following full text is a publisher's version.

For additional information about this publication click this link.

<http://hdl.handle.net/2066/174497>

Please be advised that this information was generated on 2017-12-05 and may be subject to change.

Bifurcations of Coupled Electron-Phonon Modes in an Antiferromagnet Subjected to a Magnetic Field

K. N. Boldyrev,^{1,†} T. N. Stanislavchuk,² A. A. Sirenko,² D. Kamenskiy,³ L. N. Bezmaternykh,^{4,*} and M. N. Popova¹

¹*Institute of Spectroscopy, Russian Academy of Sciences, Troitsk, Moscow 108840, Russia*

²*Department of Physics, New Jersey Institute of Technology, Newark, New Jersey 07102, USA*

³*High Field Magnet Laboratory (HFML-EMFL), Radboud University, Nijmegen 6525 ED, Netherlands*

⁴*Kirenskiy Institute of Physics, Siberian Branch of RAS, Krasnoyarsk 660036, Russia*

(Received 8 September 2016; revised manuscript received 29 December 2016; published 18 April 2017)

We report on a new effect caused by the electron-phonon coupling in a stoichiometric rare-earth antiferromagnetic crystal subjected to an external magnetic field, namely, the appearance of a nonzero gap in the spectrum of electronic excitations in an arbitrarily small field. The effect was registered in the low-temperature far-infrared (terahertz) reflection spectra of an easy-axis antiferromagnet $\text{PrFe}_3(\text{BO}_3)_4$ in magnetic fields $\mathbf{B}_{\text{ext}} \parallel c$. Both paramagnetic and magnetically ordered phases (including a spin-flop one) were studied in magnetic fields up to 30 T, and two bifurcation points were observed. We show that the field behavior of the coupled modes can be successfully explained and modeled on the basis of the equation derived in the framework of the theory of coupled electron-phonon modes, with the same field-independent electron-phonon interaction constant $|W| = 14.8 \text{ cm}^{-1}$.

DOI: 10.1103/PhysRevLett.118.167203

A coupling between the electronic system and the lattice vibrations is responsible for a number of fundamental effects in solids such as classical superconductivity [1], different kinds of the Jahn-Teller effect [2], a splitting of degenerate phonon modes in concentrated transition-metal or rare-earth (RE) compounds under an applied external magnetic field [3–5], delocalization of the electronic states in the energy range of optical phonons, and, as a consequence, an observable electronic Davydov splitting [4,6]. The electron-phonon interaction induces ferroelectricity in many ferroelectrics [7,8] and plays an important role in the thermal and electronic conductivity of materials [9–11] as well as in energy dissipation in electronic devices [11–13]. Narrow zero-phonon spectral lines in crystals, which are useful probes of a local crystal structure and of different interactions, shift and dramatically broaden with increasing the temperature, mainly because of the electron-phonon coupling [14]. The same coupling is responsible for the crystal-field levels' relaxation and, hence, the lifetimes. The values of these effects and of the multiphonon relaxation rates (also dependent on the electron-phonon interaction) are of primary importance for laser applications, because they influence the gain, output frequency stability, and thermal tunability of a laser [14].

In the case of a resonance between a phonon and an electronic excitation, the electron-phonon interaction results in a formation of coupled electron-phonon modes [5,6,15–18]. An avoided crossing of the electronic crystal-field (CF) level of a RE ion with the acoustic phonon branch in the middle of the Brillouin zone, which is a signature of a coupled electron-phonon mode, was observed in neutron scattering experiments on TmVO_4

[16] and $\text{Tb}_2\text{Ti}_2\text{O}_7$ [17]. In optical measurements, which probe the Γ point ($\mathbf{k} = 0$) of the Brillouin zone, the resonance between an optical phonon and an electronic excitation was achieved by tuning an electronic level by an external magnetic field. In such a way, coupled electron-phonon modes were observed in Raman and infrared spectra of a number of RE-containing compounds [3–6]. An avoided crossing between a field-dependent Co^{2+} CF excitation level and low-frequency wagging phonons was observed in Raman spectra of $\text{Co}[\text{N}(\text{CN})_2]_2$ in a strong magnetic field of about 20 T [18]. The formation of coupled electron-phonon modes is typical of a very broad class of stoichiometric *f* and *d* materials, including many functional ones. It results in appreciable changes in the low-frequency energy spectrum that governs the thermodynamic and magnetic properties of the compound. That is why it is important to understand the physics of coupled electron-phonon modes and of their behavior in external magnetic fields.

In this Letter, we report on a new effect associated with the electron-phonon interaction, namely, the appearance of a nonzero gap in the spectrum of coupled electron-phonon modes in an antiferromagnetically ordered compound subjected to an arbitrarily small external magnetic field. To detect this effect, a unique experiment has been carried out, namely, low-temperature reflection measurements in the far-infrared (terahertz) spectral region and in the Voight geometry (i.e., with radiation incident onto the sample at the direction perpendicular to that of an applied external magnetic field). Magnetic fields up to 30 T were used. The effect was observed in the spectrum of a multiferroic antiferromagnetic $\text{PrFe}_3(\text{BO}_3)_4$ single crystal. Multiferroic compounds exhibit

a mutual interference of the charge, lattice, and spin degrees of freedom and are the most promising candidates for observing new effects mediated by the electron-phonon interaction. In particular, a strong resonance electron-phonon interaction resulting in coupled phonon- $4f$ -electronic excitations has recently been evidenced in multiferroic $\text{PrFe}_3(\text{BO}_3)_4$ [19] and $\text{TbFe}_3(\text{BO}_3)_4$ [20]. It is worth noting, however, that both the very existence of coupled electron-phonon modes and the effect of a gap at the bifurcation point are, by no means, limited to multiferroics.

Praseodymium and terbium iron borates crystallize into the trigonal noncentrosymmetric structure of the natural mineral huntite (space group $R32$), order into an easy-axis antiferromagnetic (AFM) structure [at 32 and 40 K for $\text{PrFe}_3(\text{BO}_3)_4$ [21,22] and $\text{TbFe}_3(\text{BO}_3)_4$ [23,24], respectively], undergo a spin-flop phase transition at which the antiferromagnetically ordered along the c axis Fe^{3+} spins flop onto the ab plane [in the magnetic field B_{SF} of 4.5 and 3.5 T for $\text{PrFe}_3(\text{BO}_3)_4$ [21] and $\text{TbFe}_3(\text{BO}_3)_4$ [23], respectively, at $T = 4.2$ K], incorporate non-Kramers RE ions that have crystal-field levels in the energy region of phonons, and belong to a new class of multiferroics [25]. Effects observed due to the $4f$ -electron-phonon interaction are particularly simple and clear for the interpretation in the case of $\text{PrFe}_3(\text{BO}_3)_4$ that preserves the $R32$ (D_3^7) structure with one formula unit in the primitive crystal cell down to the lowest temperatures and demonstrates a resonance interaction between nondegenerate electronic and lattice excitations of the same symmetry (Γ_2 and A_2 irreducible representations of the crystal factor group D_3 , in the notations accepted for electronic excitations and phonons, respectively). In contrast, $\text{TbFe}_3(\text{BO}_3)_4$ undergoes a structural phase transition (at ~ 200 K) into an enantiomorphic space-group pair $P3_121$ (D_3^4) and $P3_221$ (D_3^6) with three formula units in the primitive cell and exhibits a coupling between a doubly degenerated E phonon and two Davydov multiplets of the Γ_3 symmetry.

In $\text{PrFe}_3(\text{BO}_3)_4$, the singlet ground Γ_2 and the first excited Γ_1 (at about 49 cm^{-1}) states of the Pr^{3+} ion are well isolated from the other CF states (the next nearest CF level is at 192 cm^{-1} and has the Γ_3 symmetry [22]), and they govern the low-temperature magnetic and magnetoelectric properties of the compound [21,22,26]. The electronic CF excitation corresponding to the $\Gamma_2 \rightarrow \Gamma_1$ optical transition of Pr^{3+} strongly interacts with the lowest-frequency A_2 lattice phonon mode associated, mainly, with motions of the heavy Pr^{3+} ions, which is accompanied by a strong mixing of electronic and vibrational wave functions, energy renormalization, and redistribution of intensities in the spectrum (i.e., a coupled electron-phonon mode is formed) [19].

In the present study, we have used the same well-oriented single crystal of $\text{PrFe}_3(\text{BO}_3)_4$ as in Ref. [19]. Optical π -polarized ($\mathbf{k} \perp c$, $\mathbf{E} \parallel c$) reflection measurements in the far-infrared (terahertz) spectral region $20\text{--}100 \text{ cm}^{-1}$ ($0.6\text{--}3 \text{ THz}$) at the temperatures $1.5\text{--}50 \text{ K}$ and external

magnetic fields $\mathbf{B}_{\text{ext}} \parallel c$ up to 8 T were performed on the U4-IR beam line of the National Synchrotron Light Source, Brookhaven National Laboratory, USA, using a Fourier spectrometer Bruker IFS-66v with a liquid-helium bolometer (4.2 K) as a detector and an optical Oxford SM4000 superconducting magnet. Unpolarized reflection ($\mathbf{k} \perp c$) over the same spectral interval, at 1.5 K and in magnetic fields up to 30 T, was studied at the High Field Magnet Laboratory, Netherlands. For this study, we used a Fourier spectrometer Bruker IFS-113v combined with a 33-Tesla Bitter electromagnet. The radiation was detected using a silicon bolometer operating at 1.5 K.

Figures 1(a) and 1(c) display representative reflection spectra of $\text{PrFe}_3(\text{BO}_3)_4$ in magnetic fields $\mathbf{B}_{\text{ext}} \parallel c$ up to 8 T at the temperatures 1.5 and 40 K $> T_N = 32 \text{ K}$, respectively. The corresponding reflection intensity maps in the

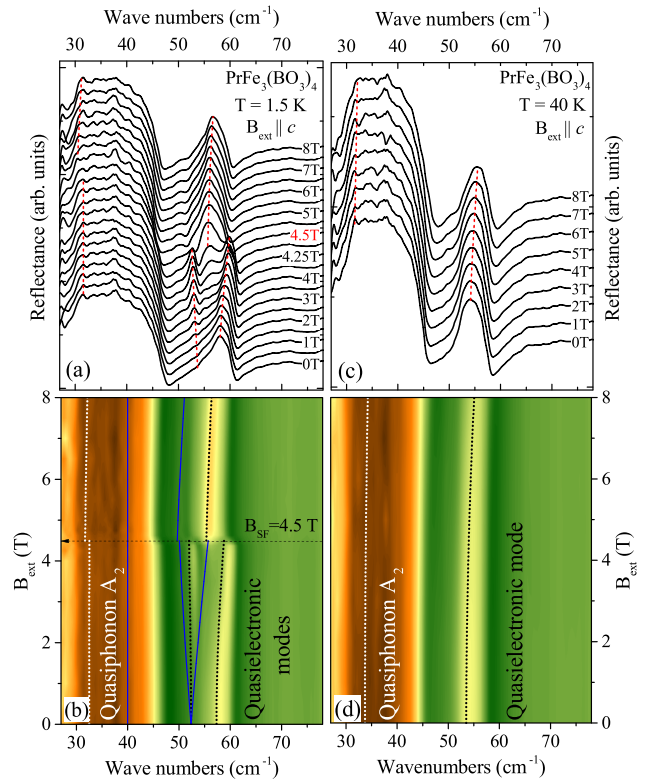


FIG. 1. The π -polarized far-infrared reflection spectra of $\text{PrFe}_3(\text{BO}_3)_4$ in external magnetic fields $\mathbf{B}_{\text{ext}} \parallel c$ up to 8 T and the corresponding reflection intensity maps [dark-brown (dark-green) color corresponds to the reflectance close to unity (zero)] as functions of the frequency and magnetic field at (a),(b) $T = 1.5 \text{ K}$ and (c),(d) $T = 40 \text{ K} > T_N = 32 \text{ K}$. The spin-flop transition in the field $B_{\text{SF}} \approx 4.5 \text{ T}$ is clearly observed in the spectra taken at 1.5 K. Blue solid lines in (b) show the field behavior of the phonon and two electronic branches [see Eq. (1)] in the absence of the electron-phonon coupling. Dotted lines represent the results of calculations according to Eqs. (1) and (2), with the following set of parameters: (a)–(d) $|W| = 14.8 \text{ cm}^{-1}$, $\omega_{\text{ph}} = 40 \text{ cm}^{-1}$, $E = 49 \text{ cm}^{-1}$, $g_0 \langle \Gamma_1 | J_Z | \Gamma_2 \rangle = 1.9$, and (a),(b) $B_{\text{int}} = 10.5 \text{ T}$ for $B_{\text{ext}} < B_{\text{SF}}$ (for details, see the text).

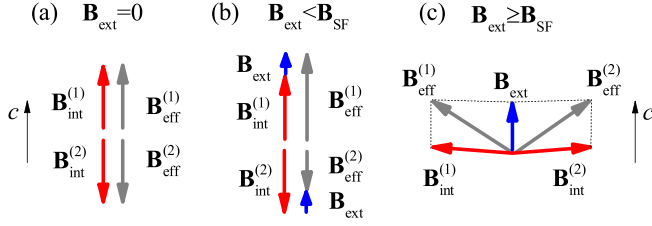


FIG. 2. Scheme illustrating the formation of an effective magnetic field at the two praseodymium subsystems in different regions of the B - T phase diagram in the case $\mathbf{B}_{\text{ext}} \parallel c$. (a) AFM phase, $B_{\text{ext}} = 0$; (b) AFM phase, $B_{\text{ext}} < B_{\text{SF}}$; (c) spin-flop phase, $B_{\text{ext}} \geq B_{\text{SF}}$.

frequency–external magnetic field axes are presented in Figs. 1(b) and 1(d). In an easy-axis antiferromagnetic state ($T = 1.5$ K, $B_{\text{ext}} < B_{\text{SF}}$), iron magnetic moments aligned along the c axis create an internal staggered magnetic field at the praseodymium sites, $\mathbf{B}_{\text{int}} \parallel c$, the value of which reaches $B_{\text{int}} \approx 10.5$ T at 1.5 K [22]. An external magnetic field $\mathbf{B}_{\text{ext}} \parallel c$, being summed with this field, results in effective magnetic fields $B_{\text{eff}}^{(i)}$, where $B_{\text{eff}}^{(1)} = B_{\text{int}} + B_{\text{ext}}$ at one-half of the praseodymium sites (Pr subsystem 1) and $B_{\text{eff}}^{(2)} = B_{\text{int}} - B_{\text{ext}}$ at the other half (Pr subsystem 2), as is shown schematically in Figs. 2(a) and 2(b). In the absence of the electron-phonon interaction, there are two electronic energy branches with energies $\omega_{\text{el},1}$ and $\omega_{\text{el},2}$ corresponding to these two Pr subsystems:

$$\omega_{\text{el},i}^2 = E^2 + 4\mu_B^2 g_0^2 |\langle \Gamma_1 | J_Z | \Gamma_2 \rangle|^2 |B_{\text{eff}}^{(i)}|^2, \quad i = 1, 2 \quad (1)$$

[here, $E = 49$ cm $^{-1}$ is the energy of the Γ_1 first excited CF level of Pr^{3+} in paramagnetic $\text{PrFe}_3(\text{BO}_3)_4$, μ_B is the Bohr magneton, and g_0 is the Landé factor]. These branches are shown by blue solid lines in Fig. 1(b). Their energies converge to the same value ω_{el} at $B_{\text{ext}} \rightarrow 0$, $\omega_{\text{el}}^2 = E^2 + 4\mu_B^2 g_0^2 |\langle \Gamma_1 | J_Z | \Gamma_2 \rangle|^2 B_{\text{int}}^2$. As is evident from Figs. 1(a) and 1(b), two experimentally observed electronic branches (in the region from 50 to 60 cm $^{-1}$) converge to different wave numbers at $B_{\text{ext}} \rightarrow 0$, which confirms once more a crucial role of the electron-phonon coupling.

To find the frequencies of coupled electron-phonon excitations in the case of a nondegenerate phonon mode with unperturbed frequency ω_{ph} and two electronic excitations having frequencies $\omega_{\text{el},1}$ and $\omega_{\text{el},2}$, one has to solve the following equation obtained on the basis of the results derived in Ref. [15] using the Green's functions method:

$$(\omega^2 - \omega_{\text{ph}}^2) - 2\omega_{\text{ph}} |W|^2 \times \left(\frac{\omega_{\text{el},1}(n_{01} - n_1)}{\omega^2 - \omega_{\text{el},1}^2} + \frac{\omega_{\text{el},2}(n_{02} - n_2)}{\omega^2 - \omega_{\text{el},2}^2} \right) = 0. \quad (2)$$

Here, W is the electron-phonon coupling constant, and n_{0i} and n_i are the relative populations of the ground and excited states, respectively, of the Pr^{3+} ions in the i th praseodymium subsystem, $i = 1, 2$. In the case of

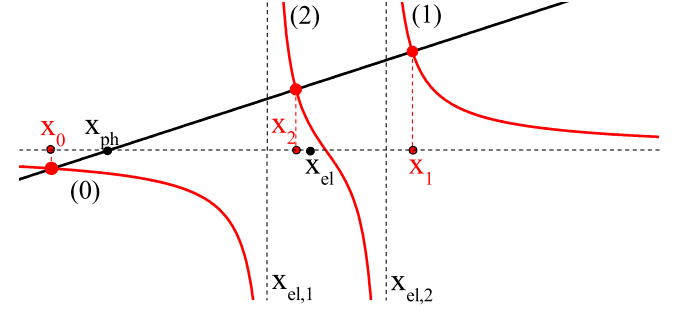


FIG. 3. Graphical solution of Eq. (3). Roots of the equation are found as abscissas of the points where the straight line crosses branches (0), (1), and (2). The branch (2) disappears in the case $x_{\text{el},1} = x_{\text{el},2}$. $x_{\text{el}} \equiv \omega_{\text{el}}^2 = E^2 + 4\mu_B^2 g_0^2 |\langle \Gamma_1 | J_Z | \Gamma_2 \rangle|^2 B_{\text{int}}^2$. For other notations, see the text.

$T = 1.5$ K considered here, $n_1 \approx n_2 \approx 0$ but $n_{01} \approx n_{02} \approx 1/2$, and we rewrite Eq. (2) in the following form:

$$(x - x_{\text{ph}}) = \sqrt{x_{\text{ph}}} |W|^2 \left(\frac{\sqrt{x_{\text{el},1}}}{x - x_{\text{el},1}} + \frac{\sqrt{x_{\text{el},2}}}{x - x_{\text{el},2}} \right), \quad (3)$$

where the notations $x_{\text{ph}} \equiv \omega_{\text{ph}}^2$ and $x_{\text{el},i} \equiv \omega_{\text{el},i}^2$ are introduced. Figure 3 presents a graphical solution of Eq. (3). The right part of the equation as a function of x consists of three branches [marked (0), (1), and (2) in Fig. 3]; they have singularities at the points $x_{\text{el},1}$ and $x_{\text{el},2}$. These branches are crossed by a straight line representing the left part of Eq. (3), at the three points x_0 , x_1 , and x_2 , which give the roots of Eq. (3). The branch (2) disappears in the case $x_{\text{el},1} = x_{\text{el},2}$, and a cubic Eq. (3) (or 2) reduces to a quadratic one. There are three situations in our experiment on $\text{PrFe}_3(\text{BO}_3)_4$ corresponding to this case, namely, (i) the AFM phase, $B_{\text{ext}} = 0$, (ii) the paramagnetic phase ($B_{\text{int}} = 0$), any B_{ext} , and (iii) the AFM spin-flop phase, $B_{\text{ext}} \geq B_{\text{SF}}$.

The first case, which corresponds to the lowest spectral trace in Fig. 1(a), has already been considered in Ref. [19]. Two reflection bands present in a zero magnetic field correspond to the two branches of a coupled $4f$ -electron-phonon mode that is formed below the temperature of ~ 100 K, at which the population of the CF level lying at about 49 cm $^{-1}$ markedly diminishes. As the temperature decreases, the high-frequency quasidelectronic branch gains its intensity at the expense of a strong low-frequency quasiphonon branch. It is worth noting that pure $4f$ -electronic excitations are not observable in the reflection spectra, due to their low oscillator strengths ($\sim 10^{-6}$ – 10^{-8}). The temperature behavior of the spectrum has been successfully modeled using Eq. (2) with $\omega_{\text{el},1} = \omega_{\text{el},2} = \omega_{\text{el}}(T)$ found from the optical measurements, the Boltzmann distribution of populations of electronic levels, $|W| = 14.8$ cm $^{-1}$, and $\omega_{\text{ph}}(T) = \omega_{\text{ph}}(300\text{K}) - 0.019(300 - T)$ with $\omega_{\text{ph}}(300\text{K}) = 45.2$ cm $^{-1}$ [19].

In the second case of a paramagnetic state of $\text{PrFe}_3(\text{BO}_3)_4$ ($T = 40$ K, $B_{\text{int}} = 0$), corresponding to

Figs. 1(c) and 1(d), an external magnetic field $\mathbf{B}_{\text{ext}}\parallel c$ shifts the first excited Γ_1 CF level to higher frequencies $\omega_{\text{el}}^2 = E^2 + 4\mu_B^2 g_0^2 |\langle \Gamma_1 | J_z | \Gamma_2 \rangle|^2 B_{\text{ext}}^2$, due to a nondiagonal Zeeman interaction with the ground Γ_2 level. Correspondingly, a gradual shift of both branches of the electron-phonon mode is observed. We model here this behavior in the frame of the same approach as in the first case, with the same set of parameters, namely, $|W| = 14.8 \text{ cm}^{-1}$, $\omega_{\text{ph}}(40 \text{ K}) = 40 \text{ cm}^{-1}$, and $E = \omega_{\text{el}}(40 \text{ K}, B_{\text{ext}} = 0) = 49 \text{ cm}^{-1}$ for the value of the electron-phonon coupling constant and unperturbed ($|W| = 0$) phonon and electronic excitation frequencies, respectively [dotted lines in Figs. 1(c) and 1(d)].

In the third case of an antiferromagnetic $\text{PrFe}_3(\text{BO}_3)_4$ subjected to an external magnetic field $\mathbf{B}_{\text{ext}}\parallel c$ with the strength above that of a spin-flop transition, $B_{\text{ext}} \geq B_{\text{SF}} = 4.5 \text{ T}$ ($T = 1.5 \text{ K}$), the largest component of an internal magnetic field from the iron subsystem is in the ab plane [see Fig. 2(c)] and does not influence the Pr subsystem (because of zero matrix elements of the operators J_x and J_y between the states Γ_1 and Γ_2 of Pr^{3+}). The z component of the internal magnetic field, as estimates based on the magnetization data of Ref. [21] show, is much smaller than B_{ext} at any B_{ext} in the interval between B_{SF} and 30 T. As a result, the behavior of all praseodymium ions in the spin-flop phase is governed by $\mathbf{B}_{\text{ext}}\parallel c$. Again, a successful modeling is achieved for the frequencies of the two branches of a coupled electron-phonon mode of $\text{PrFe}_3(\text{BO}_3)_4$ ($T = 1.5 \text{ K}$) in an external magnetic field parallel to the c axis and having a strength from 4.5 to 22 T (for the high-field behavior, see Fig. 4). As the external field grows, the energy gap between the electronic level and the considered lattice phonon mode also grows, the interaction between two excitations weakens, and the quasiaelectronic mode gains less intensity from the quasisphonon mode, until it disappears in the spectrum at fields above $\sim 22 \text{ T}$ (see Fig. 4). Weak traces of the quasiaelectronic mode appear again above $\sim 25 \text{ T}$ when this mode approaches the lowest-frequency E phonon mode. A weak interaction between these two excitations can take place because of an admixture of wave functions of the Γ_3 CF level at 192 cm^{-1} to the Γ_1 wave functions by the ab component of the internal magnetic field at the Pr sites in the spin-flop phase. The magnetic structure of the compound does not change in the range of fields $B_{\text{SF}} < B_{\text{ext}} < 30 \text{ T}$ that are weaker than the Fe-Fe exchange field $B_{\text{Fe-Fe}} \sim 100 \text{ T}$ [26]. It is worth noting the fact that the same electron-phonon coupling constant $|W| = 14.8 \text{ cm}^{-1}$ is valid throughout a broad range of magnetic fields from zero to 30 T, though a field could, in general, influence matrix elements entering W and, thus, alter the latter. The experiment with the fields up to 30 T enabled us to find a precise value of the matrix element $\langle \Gamma_1 | J_z | \Gamma_2 \rangle$; namely, the value $g_0 \langle \Gamma_1 | J_z | \Gamma_2 \rangle = 1.9$ gave the best agreement with the experimental data.

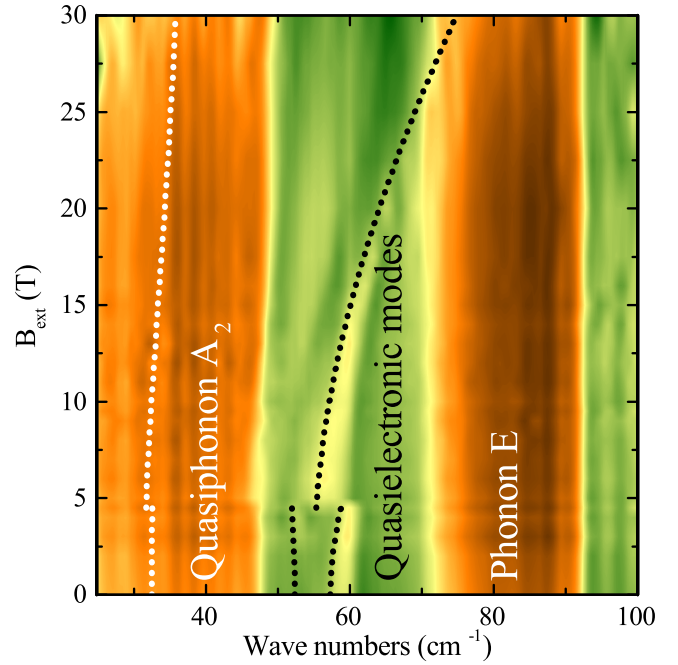


FIG. 4. Unpolarized far-infrared reflection intensity maps for $\text{PrFe}_3(\text{BO}_3)_4$ in external fields $\mathbf{B}_{\text{ext}}\parallel c$ up to 30 T, at $T = 1.5 \text{ K}$. Dotted lines represent results of calculations according to Eqs. (1) and (2), with the following set of parameters: $|W| = 14.8 \text{ cm}^{-1}$, $\omega_{\text{ph}} = 40 \text{ cm}^{-1}$, $E = 49 \text{ cm}^{-1}$, and $g_0 |\langle \Gamma_1 | J_z | \Gamma_2 \rangle| = 1.9$.

In the case of the electron-phonon coupling in an easy-axis antiferromagnet subjected to an external magnetic field directed along the easy axis, two bifurcation points are present in the spectra of excitations, as can be seen in Figs. 1(a) and 1(b). The first one corresponds to an application of a magnetic field $B_{\text{ext}} \neq 0$, which immediately converts a quadratic equation for the coupled electron-phonon modes into a cubic one. A new excitation in the spectrum appears with the frequency $\omega_2^2 \equiv x_2 < x_{\text{el}} \equiv \omega_{\text{el}}^2 = E^2 + 4\mu_B^2 g_0^2 |\langle \Gamma_1 | J_z | \Gamma_2 \rangle|^2 B_{\text{int}}^2$. At $B_{\text{ext}} \rightarrow 0$, $x_2 \rightarrow x_{\text{el}}$, whereas the root x_1 that existed at $B_{\text{ext}} = 0$ tends to $x_{\text{el}} + O(|W|)$, so that $x_1 > x_{\text{el}}$ at any $|W| \neq 0$. Thus, at any $|W| \neq 0$ and $0 < B_{\text{ext}} < B_{\text{SF}}$, there are two quasiaelectronic branches in the spectrum of coupled modes in the easy-axis AFM phase of $\text{PrFe}_3(\text{BO}_3)_4$, with a gap between them. While the “old” high-frequency quasiaelectronic branch almost does not change its intensity with a growing magnetic field, the “new” low-frequency one gradually gains its intensity. This behavior of intensities demands a special consideration, which is out of scope of the present Letter. The second bifurcation point is at B_{SF} . Diminishing of B_{ext} below this value abruptly transforms the quadratic Eq. (2) (with $\omega_{\text{el},1} = \omega_{\text{el},2}$) into the cubic one [Eq. (2), $\omega_{\text{el},1} \neq \omega_{\text{el},2}$], and one quasiaelectronic excitation splits into two with abrupt frequency jumps.

In summary, we have performed a spectroscopic investigation of an easy-axis antiferromagnet $\text{PrFe}_3(\text{BO}_3)_4$ in magnetic fields $\mathbf{B}_{\text{ext}}\parallel c$ up to 30 T, in the far-infrared region

that includes frequencies of a praseodymium electronic nondegenerate crystal-field excitation of the Γ_2 symmetry and the lattice phonon mode of the same symmetry. An interaction between these two excitations results in a formation of coupled $4f$ -electron-phonon modes. The field behavior of these coupled modes was studied in a paramagnetic (at $T = 40$ K), easy-axis antiferromagnetic ($T = 1.5$ K, $B_{\text{ext}} < B_{\text{SF}} = 4.5$ T), and a spin-flop ($T = 1.5$ K, $B_{\text{ext}} \geq B_{\text{SF}}$) phase. We show that in the three cases, namely, (i) the AFM phase in a zero external field, (ii) the paramagnetic phase in any field, and (iii) the AFM spin-flop phase, the field behavior can be successfully modeled on the base of a quadratic equation derived in the frame of the theory of coupled electron-phonon modes, with one field-independent set of parameters. In the case of the easy-axis AFM phase ($T = 1.5$ K, $0 < B_{\text{ext}} < B_{\text{SF}}$), the quadratic equation converts into a cubic one and bifurcations corresponding to an abrupt appearance of the third root are observed in the terahertz reflection spectra at the two bifurcation points, $B_{\text{ext}} = B_{\text{SF}}$ and $B_{\text{ext}} = +0$. Again, the field behavior of the coupled modes is successfully simulated using the same set of parameters. The field behavior of the spectrum of excitations differs qualitatively from the behavior in the absence of electron-phonon coupling; in particular, a nonzero energy gap between two electronic modes exists at an arbitrarily small external magnetic field. This discovered new effect can take place in any easy-axis antiferromagnet, provided that phonon and electronic excitations are positioned close enough (accidentally or by tuning with an external field).

In conclusion, our work shows a new nontrivial manifestation of electron-phonon interaction in solids and explains it in an elegant way using a relatively simple model.

This research was supported by the Russian Scientific Foundation under Grant No. 14-12-01033, the President of Russian Federation (MK-3577.2017.2, K. N. B.), and the U.S. Department of Energy under Grant No. DE-FG02-07ER46382 (experiments at U4-IR beam line NSLS-BNL, T. N. S. and A. A. S.). The National Synchrotron Light Source is operated as a user facility for the U.S. Department of Energy under Contract No. DE-AC02-98CH10886. Part of this work was supported by EMFL (Contract No. 26211). M. N. P. thanks B. Z. Malkin and A. V. Popov for helpful discussions.

*Deceased.

†Corresponding author.

kn.boldyrev@gmail.com

- [1] J. Bardeen, L. N. Cooper, and J. R. Schrieffer, *Phys. Rev.* **108**, 1175 (1957).
 [2] *The Jahn-Teller Effect*, edited by H. Köppel, D. R. Yarkony, and H. Barentzen (Springer, Berlin, 2009), Springer Series in Chem. Physics Vol. 97.

- [3] K. Ahrens and G. Schaack, *Phys. Rev. Lett.* **42**, 1488 (1979).
 [4] M. Dahl and G. Schaack, *Phys. Rev. Lett.* **56**, 232 (1986).
 [5] A. K. Kupchikov, B. Z. Malkin, A. L. Natadze, and A. I. Ryskin, *Fiz. Tverd. Tela (Leningrad, USSR)* **29**, 3335 (1987) *Sov. Phys. Solid State* **29**, 1913 (1987).
 [6] J. Kraus, W. Görlitz, M. Hirsch, R. Roth, and G. Schaack, *Z. Phys. B* **74**, 247 (1989).
 [7] N. Kristoffel and P. Konsin, *Ferroelectrics* **6**, 3 (1973).
 [8] S. Fatale, S. Moser, J. Miyawaki, Y. Harada, and M. Grioni, *Phys. Rev. B* **94**, 195131 (2016).
 [9] J. M. Ziman, *Electrons and Phonons: The Theory of Transport Phenomena in Solids* (Oxford University Press, New York, 2001).
 [10] M. Lundstrom, *Fundamentals of Carrier Transport* (Cambridge University Press, Cambridge, England, 2009).
 [11] B. Liao, A. A. Maznev, K. A. Nelson, and G. Chen, *Nat. Commun.* **7**, 13174 (2016).
 [12] E. Pop, *Nano Res.* **3**, 147 (2010).
 [13] J. C. H. Chen, Y. Sato, R. Kosaka, M. Hashisaka, K. Muraki, and T. Fujisawa, *Sci. Rep.* **5**, 15176 (2015).
 [14] B. Z. Malkin, in *Spectroscopic Properties of Rare Earths in Optical Materials*, Springer Series in Materials Science Vol. 83, edited by G. Liu and B. Jacquier (Springer, New York, 2005), pp. 130–190.
 [15] A. K. Kupchikov, B. Z. Malkin, D. A. Rzaev, and A. I. Ryskin, *Fiz. Tverd. Tela (Leningrad, USSR)* **24**, 2373 (1982) *Sov. Phys. Solid State* **24**, 1348 (1982).
 [16] J. K. Kjems, W. Hayes, and S. H. Smith, *Phys. Rev. Lett.* **35**, 1089 (1975).
 [17] T. Fennell, M. Kenzelmann, B. Roessli, H. Mutka, J. Ollivier, M. Ruminy, U. Stuhr, O. Zaharko, L. Bovo, A. Cervellino, M. K. Haas, and R. J. Cava, *Phys. Rev. Lett.* **112**, 017203 (2014).
 [18] T. V. Brinzari, J. T. Haraldsen, P. Chen, Q.-C. Sun, Y. Kim, L.-c. Tung, A. P. Litvinchuk, J. A. Schlueter, D. Smirnov, J. L. Manson, J. Singleton, and J. L. Musfeldt, *Phys. Rev. Lett.* **111**, 047202 (2013).
 [19] K. N. Boldyrev, T. N. Stanislavchuk, A. A. Sirenko, L. N. Bezmaternykh, and M. N. Popova, *Phys. Rev. B* **90**, 121101 (R) (2014).
 [20] S. A. Klimin, A. B. Kuzmenko, M. A. Kashchenko, and M. N. Popova, *Phys. Rev. B* **93**, 054304 (2016).
 [21] A. M. Kadomtseva, Yu. F. Popov, G. P. Vorob'ev, A. A. Mukhin, V. Yu. Ivanov, A. M. Kuz'menko, and L. N. Bezmaternykh, *JETP Lett.* **87**, 39 (2008).
 [22] M. N. Popova, T. N. Stanislavchuk, B. Z. Malkin, and L. N. Bezmaternykh, *Phys. Rev. B* **80**, 195101 (2009).
 [23] E. A. Popova, D. V. Volkov, A. N. Vasiliev, A. A. Demidov, N. P. Kolmakova, I. A. Gudim, L. N. Bezmaternykh, N. Tristan, Yu. Skourski, B. Büchner, C. Hess, and R. Klingeler, *Phys. Rev. B* **75**, 224413 (2007).
 [24] C. Ritter, A. Balaev, A. Vorotynov, G. Petrakovskii, D. Velikanov, V. Temerov, and I. Gudim, *J. Phys. Condens. Matter* **19**, 196227 (2007).
 [25] A. I. Popov, D. I. Plokhov, and A. K. Zvezdin, *Phys. Rev. B* **87**, 024413 (2013).
 [26] N. V. Kostyuchenko, A. I. Popov, and A. K. Zvezdin, *Fiz. Tverd. Tela (St. Petersburg, Russia)* **54**, 1493 (2012) *Phys. Solid State* **54**, 1591 (2012).